www.czasopisma.pan.pl PAN POLSKA AKADEMIA NAUK www.journals.pan.pl

Arch. Min. Sci. **63** (2018), 3, 747-765

Electronic version (in color) of this paper is available: http://mining.archives.pl

DOI 10.24425/123695

ANTONI TAJDUŚ*#, MAREK CAŁA*, KRZYSZTOF TAJDUŚ**

SEISMICITY AND ROCK BURST HAZARD ASSESSMENT IN FAULT ZONES: A CASE STUDY

ZAGROŻENIE WSTRZĄSAMI I TĄPANIAMI W REJONIE USKOKÓW NA PRZYKŁADZIE WYBRANEJ KOPALNI

The coal exploitation in the Upper Silesia region (along the Vistula River) triggers the strata seismic activity, characterized by very high energy, which can create mining damage of the surface objects, without any noticeable damages in the underground mining structures. It is assumed that the appearance of the high energy seismic events is the result of faults' activation in the vicinity of the mining excavation. This paper presents the analysis of a case study of one coal mine, where during exploitation of the longwall panel no. 729, the high energy seismic events occurred in the faulty neighborhood. The authors had analyzed the cause of the presented seismic events, described the methods of energy decreasing and applied methods of prevention in the selected mining region. The analysis concluded that the cause of the high energy seismic events, during the exploitation of the longwall panel no. 729 was the rapid displacements on the fault surface. The fault's movements arose in the overburden, about 250 m above the excavated longwall panel, and they were strictly connected to the cracking of the thick sandstone layer.

Keywords: rockburst, seismic events, longwall panel, underground mining

Eksploatacja pokładów węgla w rejonie nadwiślańskim Górnego Śląska wywołuje aktywność sejsmiczną górotworu przejawiającą się wstrząsami o bardzo wysokich energiach, które nie powodują szkód w wyrobiskach górniczych, lecz są silnie odczuwane na powierzchni terenu w postaci znacznych drgań powierzchni często prowadzących do uszkodzeń obiektów budowlanych. Prognozuje się, że występowanie wstrząsów o wysokich energiach jest wynikiem uaktywnienia się uskoków spowodowanych eksploatacją prowadzoną w ich pobliżu. Podczas eksploatacji ściany 729 w sąsiedztwie uskoku również wystąpiły wstrząsy o bardzo wysokich energiach. W artykule dokonano analizy przyczyn występowania tych wstrząsów, opisano sposoby zmniejszenia energii wstrząsów i zapobiegania wystąpieniu tąpnięcia w rejonie tej ściany. Z przeprowadzonych analiz wynika, że przyczyną występowania wstrząsów o bardzo wysokich energiach podczas eksploatacji ściany 729 są nagłe przemieszczenia na uskoku

* AGH UNIVERSITY OF SCIENCES AND TECHNOLOGY, FACULTY OF MINING AND GEOENGINEERING, AL. MICKIEWICZA 30, 30-059 KRAKÓW, POLAND

** STRATA MECHANICS RESEARCH INSTITUTE OF THE POLISH ACADEMY OF SCIENCES, UL. REYMONTA 27, 30-059 KRAKOW, POLAND

Corresponding author: tajdus@agh.edu.pl

zachodzące w nadkładzie około 250 m nad eksploatowaną ścianą połączone z pękaniem grubej warstwy piaskowca.

Słowa kluczowe: tąpania, zjawiska sejsmiczne, eksploatacja ścianowa, górnictwo podziemne

1. Introduction

Rock bursts are a very common hazard in underground mining, worldwide (Coughlin & Kranz, 1991; Knoll & Kuhnt, 1990). For many years now, the exploitation of the coal in the Polish region of Upper Silesia, which includes the mines „A", „B", „C" and „D", has been causing seismic activity of the rock mass, which manifests itself through high-energy mining originated seismic shocks, which do not cause damage in the underground workings but are strongly felt on the surface, in the form of powerful ground vibrations, which often lead to the damage of buildings. One of the principle factors of the occurrence of high-energy events exceeding seismic energy level 10^7 J is the activation of faults caused by nearby mining activity (Mutke et al., 2015) . Table 1 shows the number of these events recorded since 1985 in the "**A**", "**B**", "**C**" and "**D**" coal mines.

TABLE 1

Seismic events exceeding energy level 10^7 J recorded since 1985 in the "**A**", "**B**", "**C**" and "**D**" coal mines

Name of the mine	Mining depth	Number of excavated coal seams	Number of events	Seismic energy of events	Mining conditions
„**A**"	675 m÷735 m	209	22	10^7J	Mining activity in a fault zone, hypocentres of seismic events in sandstone layers located significantly above the seam
			6	10^8J	
			1	10^9J	
„**B**"		207, 209	9	10^7J	
„**C**"	565, 700 m	207, 209	7	10^7J	
„**D**"	640 m	207	3	10^7J	
			2	10^8J	
			1	10^9J	

The goal of the present study is to determine the causes of the high-energy events, which had occurred during the exploitation of the longwall panel no. 729 in the seam no. 207 excavated in "**D**" coal mine, which was subjected to detailed observation. Each hazard related to high-energy seismic activity was analyzed, and appropriate actions were taken to enable safe mining operation.

2. Seismicity hazard in the "D" mine

Until recently, the "**D**" coal mine was considered to be a mine not threatened by strong seismic events or rock bursts. The exploitation was carried out in the seams located at depths not exceeding 500 m and during the exploitation seismic activity of the rock mass was not detected. It was for that reason that they were classified as not threatened with rock burst.

The undertaking of mining activity at a depth greater than before (640 m) in seam 207 and located in a fault zone with large throws, caused a significant increase in seismicity and

the occurrence of rock burst hazard. It appeared during the exploitation in sectors G and S_3 and particularly, during the exploitation of the longwall panel no. 729 in sector S_1. Table 2 shows the number of events and their energy rates, which had occurred during the exploitation of seam 207 in sectors G, S_3 and S_1 (Fig. 1).

TABLE 2

Number of seismic events which occurred during the exploitation of seam 207 in sectors G, S_3 and S_1

Seam 207		Number of events, N							Sum N	Cumulative seismic energy
Sector	Longwall no.	10^3 [J]	10^4 [J]	10^5 [J]	10^6 [J]	10^7 [J]	10^8 [J]	10^9 [J]	[-]	[J]
G	700	166	69	16	5	1	0	0	257	$5.4 \cdot 10^7$
	701	238	183	59	3	0	0	0	483	$4.9 \cdot 10^7$
	702	643	377	173	18	0	0	0	1211	$1.45 \cdot 10^8$
S_3	704	173	73	34	2	0	0	0	282	$1.90 \cdot 10^7$
	703	54	38	21	0	0	0	0	113	$7.7 \cdot 10^6$
S_1	729	498	299	105	6	2	2	1	913	$2.62 \cdot 10^9$
Sum		1772	1039	408	34	3	2	1	3259	$2.90 \cdot 10^9$

3. Analysis of the causes of large magnitude seismic events in longwall 729 in sector S_1

The boundaries of sectors G, S_3 and S_1 are restricted by faults with large throws, as shown in Figure 1. Inside each sector, there are numerous faults with small throws which do not exceed a few meters. The direction of these faults is either parallel or perpendicular to the direction of the central fault with large throws. The exploitation of the longwall panel no. 729 in sector S_1 was carried out along the fault with the throw of 40 m, hereby called the "north" fault (Fig. 1). During the exploitation of the longwall 729 in the vicinity of the fault, a significant seismic activity, characterized by high seismic energy events (reaching 10^9 J) was recorded. For this reason, the decision was made to carry out a detailed analysis of the causes of this phenomenon.

3.1. Description of the geological and mining conditions of sector S_1

The boundaries of sector S_1, in which the longwall panel 729 is located, are restricted by the following faults:

- from the north – the "north" fault in approximately the W-E direction and throw $h = 30 \div 50$ m in the N direction,
- from the west – the fault "west" in the NNW-SSE direction and throw $h \sim 100$ m in the SWW direction,
- from the east – the "central" fault in the NNW-SSE direction and throw $h \sim 90 \div 200$ m in the NEE direction,
- from the south – the fault in the SW-NE direction and throw $h \sim 1.4 \div 7.0$ m in the NW direction.

Seam 207, which was being exploited, lies along the NE-SW axis. It consists of a single layer of coal 3.5 m to 4.3 m thick with an average compressive (R_c) and tensile strength (R_r) equal to:

- R_c = 8.96 MPa, R_r = 0.58 MPa (in situ tests),
- R_c = 20.10 MPa, R_r = 1.58 MPa (laboratory testing).

Furthermore, an uniaxial compression test was performed on 20 samples, where the rock burst proneness index was estimated: W_{ET} = 3.20 (Kidybiński, 1981; Guo et al., 2017).

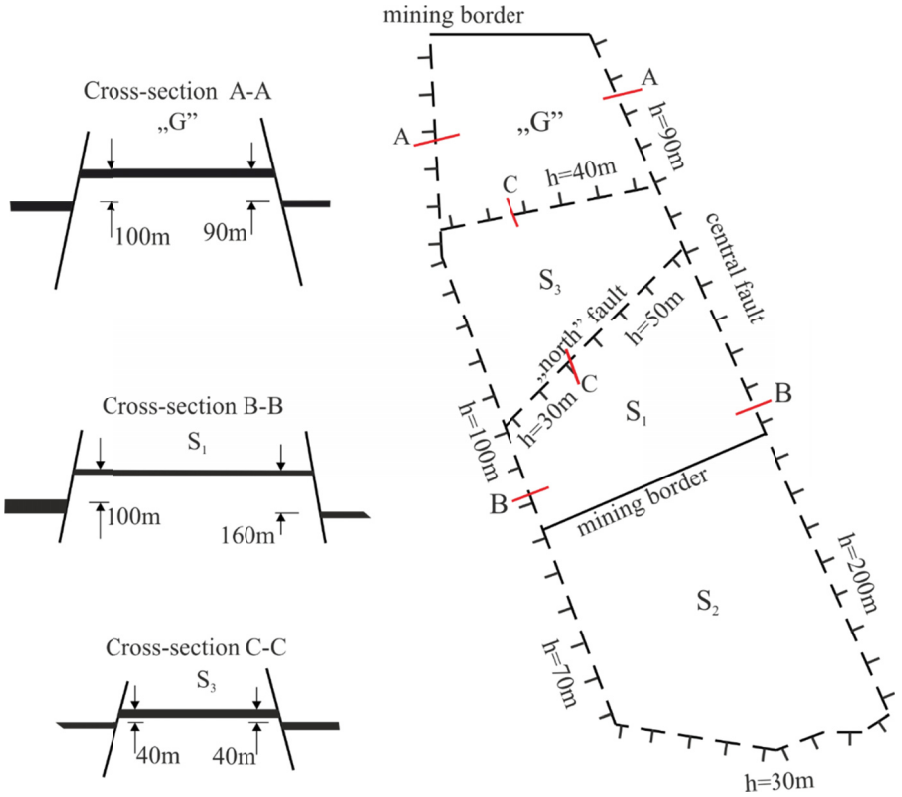

Fig. 1. The boundaries of sectors G, S_3 and S_1 are delimited by faults with large throws

In the floor, directly under seam 207, lies a layer of siltstone with a thickness of 1.70 m and beneath it lies a layer of multi-grained sandstone, which is about 66 m thick. The average value of the compressive and tensile strength for those layers was estimated in situ tests:

- shale: R_c = 22.75 MPa, R_r = 1.46 MPa,
- sandstone: R_c = 15.72 MPa, R_r = 1.01 MPa.

The direct roof has a thickness of around 4.5 m and is composed of thin layers of siltstone, sandstone and shale, with the following strength values:

- shale: R_c = 12.0 MPa, R_r = 0.77 MPa,
- sandstone: R_c = 12.92 MPa, R_r = 0.83 MPa.

In the overburden, apart from the layers of shale, mudstone, and thin layers of coal, four layers of coarse sandstone with a substantial thickness can be distinguished. Those layers are susceptible to energy accumulation:

a) layer I with thickness: $g_1 = 24$ m, lying $l_1 = 4.5$ m above seam 207,
b) layer II with thickness: $g_2 = 51$ m, lying $l_2 = 30$ m above seam 207,
c) layer III with thickness: $g_3 = 62$ m, lying $l_3 = 90$ m above seam 207,
d) layer IV with thickness: $g_4 = 90$ m, lying $l_4 = 295$ m above seam 207.

In addition to the above, two layers of sandstone can be distinguished, the thickness of which does not exceed 20 m.

Therefore, starting at the roof of seam 207, up to depth of 250 m from the surface (i.e. on the distance 385 m) the overburden consists of 70% sandstone layers, which are responsible for the high-seismic energy events. Tertiary formations, in the form of impermeable Miocene rocks (mainly silt and shale) lie at a depth of a few meters, up to 85m below the surface. Quaternary formations, mainly composed of multi-grained sands and filled with local pockets of clay and silt, can be found near the surface. The thickness of the Quaternary layer in the exploited area is small and spans between 1.3 m and 5.0 m. Such a small thickness of the quaternary and tertiary layers has a significant influence on the propagation of elastic waves following seismic events.

4. Description of seismic event with energy $9.0 \cdot 10^8$ J

Exploitation of the longwall panel 729 had caused six events of extremely large seismic energy, varying from 10^7 J to 10^9 J. The previous experience in the mining region indicated that such high energy events are very rare and regional in nature. The progress and consequences of all of these events were similar, therefore only one of them ($9.0 \cdot 10^8$ J) is described in this paper. The above mentioned seismic event occurred on September 30th, 2015 at 11:13AM and its source was located 20 m behind the longwall panel 729 and 120 m to the north-west of the "north" fault (105 m from gallery S-763). This event did not cause any damage to the excavations in the area of the longwall 729, but generated ground vibrations, recorded by the AMAX-GSI instrument:

- at a distance of 1499 m from the epicentre, the measured velocity and accelerations were V = 0.0663 m/s and A = 1.635 m/s^2 respectively,
- at a distance of 4945 m from the epicentre the velocity and accelerations were V = 0.1420 m/s and A = 0.0066 m/s^2 respectively.

The vibrations generated by this event have caused damage to buildings, which was promptly noted by the local population. Eighteen reports of damages and endangering buildings' safety were submitted (damages to chimneys, collapse of front walls, damage to gas infrastructure) as well as around 40 reports of minor damages to building structure (wall cracks, damage to household appliances, etc.). The run of the longwall face was equal to 300 m until the seismic event appeared. The location of the epicentre is illustrated in Figure 2.

The causes of the rock burst were likely to be due to:

- a significant change in the initial state of stress arose from the neighborhood of large throws' fault,
- the mining activity in the vicinity of the active "north" fault, as indicated by geophysical tests,
- the presence of thick layers of sandstones in the overburden.

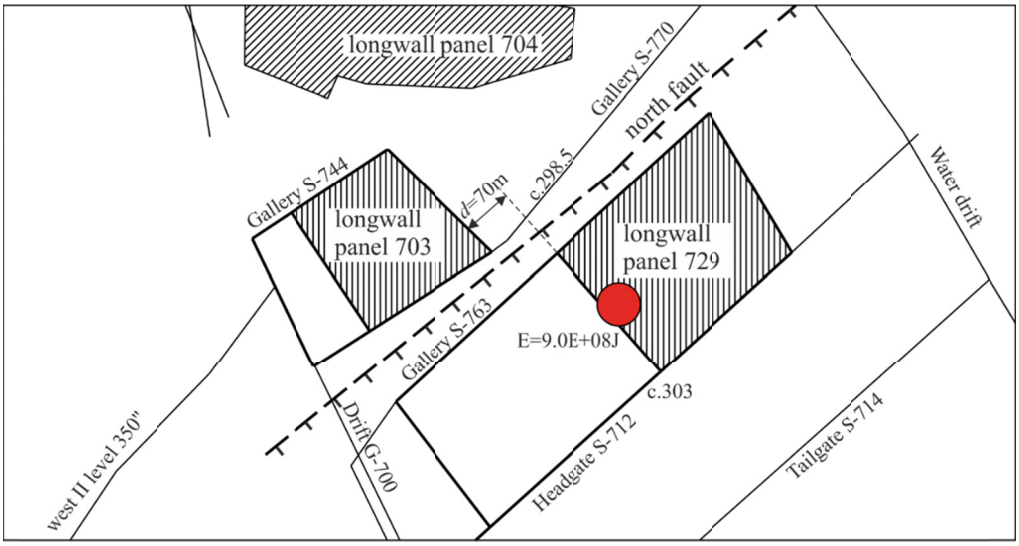

Fig. 2. Location of rock burst with energy $9.0 \cdot 10^8$ J on September 30th, 2015

5. Analysis of the rock mechanics causes of seismic events with extremely large energy

5.1. Estimation of the initial state of stress in part S_1 in the vicinity of longwall 729

The faults with large throws were shown in figure 1 and basing on this, the location of the sector S_1 was defined as the region between the footwall side of "north" fault with an average throw of 40 m (normal fault) and the hanging wall of the "central" fault. The discontinuities (i.e. the "central" fault from the east and from the west) elevated the sector S_1 with respect to the surrounding areas. The "north" fault is the so-called normal fault.

It is assumed that in a rock mass without tectonic disturbances, the initial state of stress can be determined from the following equations:

$$p_z = -\gamma_{sr} \cdot H \qquad \text{and} \qquad p_x = \gamma \cdot p_z \tag{1}$$

where, $\lambda = \dfrac{\nu}{1-\nu}$ (ν – Poisson coefficient).

For the exploitation carried out on the seam 207 at a depth of $H = 640$ m, the values for the initial state of stress are: $p_z = 16$ MPa, $p_x = p_y = 5.3$ MPa (for $\nu = 0.25$ and $\lambda = 0.33$).

Tajduś et al. (2016) analyzed the state of the stress in the vicinity of the normal fault. Basing on it, the following conclusions were made:

- the value of vertical stress p_z^u is close to the value p_z estimated for seams without faults $p_z = p_z^u = 16$ MPa,

- in the footwall at a depth of 640 m, the horizontal stresses in the vicinity of the fault p_x^u and in direction perpendicular to it are about $p_x^u = -15.0$ MPa ($\lambda = 0.94$),
- in the footwall at a depth of 640 m, the horizontal stresses near the fault parallel direction are $p_y^u = -9.7$ MPa ($\lambda = 0.61$).

The estimated horizontal values of the initial state of stress occurring in the vicinity of longwall 729 along the fault can be one of the reasons for the seismic activity in the rock mass during the excavation of the panel. However, seismic events with extremely large seismic energy must have another cause, especially given the ground effects.

5.2. 3D numerical calculations for the exploitation of the wall 729, lead parallel to the fault

To calculate the influence of the existence of the 'north' fault on the stress field in the region of the 729 wall, exploited in the seam 209, a 3D numerical model was built. Inside the model, a plane of a normal fault with a 68° slope and a throw of 45 m was located. Friction may be present at the surface of the fault.

It was assumed that in a footwall, the thickness of coal seam is 4.0 m and is located at the depth of 640 m. The direct roof consist of 5 m layer of shale and above it there is a layer of hard sandstone, with is 24 m thickness. Both the upper and the lower parts of the model are built out of shale. It was assumed that the layers behave as an elastic medium with the values present in table 3.

TABLE 3

Modelled rock mass properties

Layers	Rock properties		
	E [GPa]	ν	Density ρ [kg/m^3]
Shale	5.0	0.25	2,500
Coal	2.5	0.30	1,600
Sandstone	15.0	0.12	2,500
Rock in the caved zone	0.2	0.40	2,100
Rock in the fractured zone	0.5	0.35	2,300

The numerical model (Fig. 3) is built out of 810 thousands of six walled zones (from Finite Element Method), and 4900 contact elements of the Goodman type. The longwall excavation with caving in this model was stimulated through the removal of elements in the working space and the change of the elastic properties of the elements in both the caved and fractured zone, in accordance with the data in table 3. It was assumed that at the fault, the value of the friction coefficient equals $\mu = 1.0$.

The analysis of fault influence on the mining conditions was made for an example of longwall panel excavation with a length 220 m located alongside the fault. Three variants were considered:

(1) exploitation 40 m away from the fault,
(2) exploitation 20 m away from the fault,
(3) exploitation 5 m away from the fault.

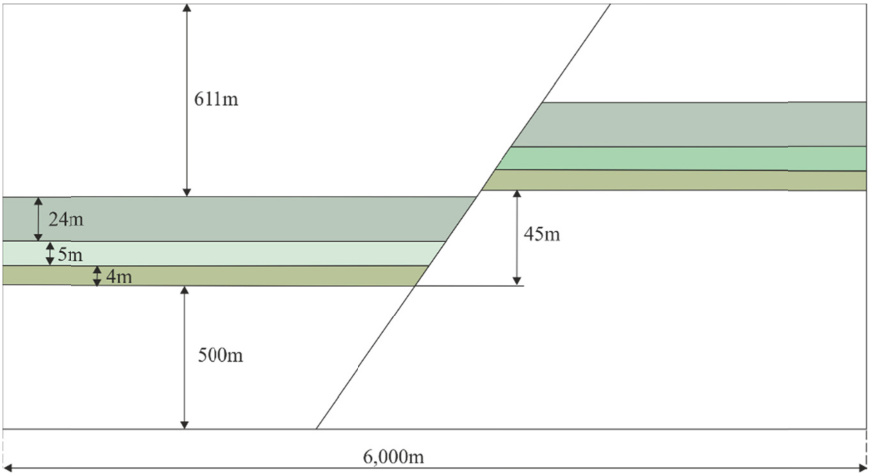

Fig. 3. Scheme of the numerical model

Excavations of the longwall panel were modelled for every 100 m. Due to the large amount of calculations' results received, table 4 includes only the values for a cross-section located 50 m above the exploited longwall (depth 590 m). At this depth, the initial state of the stress, without taking the existence of the fault into account, amounted to p_z = 14.75MPa, $p_x = p_y$ = 4.87 MPa, but considering the fault zone the values of stresses perpendicular p_{up} and parallel p_{sp} to the inclined fault plain (α_u = 68°) can be estimated from the following formulas[1]:

$$p_{up} = \frac{p_z + p_x}{2} + \frac{p_z - p_x}{2}\cos(2\alpha_u)$$

$$p_{us} = \frac{p_z - p_x}{2}\sin(2\alpha_u)$$

The results of the calculations presents that p_{up} = 6.26 MPa and p_{us} = 3,43 MPa.

Table 4 shows the results in the form of the maximum values of the stress, as compared to the initial stresses.

TABLE 4

Distance from the fault	Longwall panel run											
	100 m				300 m				500 m			
	$\frac{\sigma_x^{max}}{p_x}$	$\frac{\sigma_z^{max}}{p_z}$	$\frac{\sigma_{up}^{max}}{p_{up}}$	$\frac{\tau_{us}^{max}}{p_{us}}$	$\frac{\sigma_x^{max}}{p_x}$	$\frac{\sigma_z^{max}}{p_z}$	$\frac{\sigma_{up}^{max}}{p_{up}}$	$\frac{\tau_{us}^{max}}{p_{us}}$	$\frac{\sigma_x^{max}}{p_x}$	$\frac{\sigma_z^{max}}{p_z}$	$\frac{\sigma_{up}^{max}}{p_{up}}$	$\frac{\tau_{us}^{max}}{p_{us}}$
40 m	1.22	1.63	1.86	1.58	1.43	1.84	2.03	1.59	1.44	1.88	2.07	1.59
20 m	1.27	1.63	2.14	2.10	1.48	1.85	2.40	2.33	1.49	1.89	2.44	2.40
5 m	1.32	1.64	2.31	2.56	1.51	1.86	2.73	3.00	1.52	1.90	2.78	3.11

[1] Calculations are necessary to compare the state of the stress at the fault with the initial state of the stress.

Basing on the analysis of all the results achieved, the following conclusions can be formulated:

- The increase the longwall panel run by around 300 m creates the growth of stress concentration, which, along with the increase of the ratio of the exploitation panel, practically stabilise. This conclusion is confirmed by the observations during the excavation of longwall 729, where the first large seismic event occurred for the panel run equal 260 m.
- Along with the decrease of the width of the pillar between the exploited longwall and the fault, a very significant increase in the concentration of the stresses which occur on the surface of the fault (both shear and normal) is observed. Contrary to the initial predictions, the increase is quite small in the exploited longwall itself. Very high gradients of stresses both shear and normal (close to a threefold increase) indicate that there is a serious threat to the fault's stability, from the longwall that is excavated closer than 40 m from the fault. The distribution of stress both shear and normal along the fault is uneven. At the fault below the exploited longwall, there is a significant relaxation, but at the level of the exploited longwall and above, there is a large concentration of shear and normal stresses. This leads to the conclusion that the tremors of the rock mass occur at the fault significantly higher than the exploited wall, which is confirmed by observations. The pillar between the longwall and the fault should not be smaller than 40 m.

5.3. Geomechanical factors at play during exploitation of longwall 729

The longwall panel no. 729 is 220 m wide and of average length: 630 m. Three zones are formed above it: caved (h_z), fracture (h_s) and bending (h_u). The total height of the caved and fracture zones (Staroń, 1979; Peng, 2006) for an average seam thickness of $g = 4$ m can be estimated as 32m for a bulking factor equal to $k = 1.25$ ($h_z + h_s = \frac{2g}{k-1}$). The value of the bulking factor was estimated by taking under consideration the low strength parameters of rocks in the seam roof and its stratification. Some researchers believe that the height of the caved zone is two to three times greater than the value computed above (Borisow, 1980). The height of the caved and fracture zones indicates that a cyclical breaking of layer I of sandstone occurs during excavation which, together with the rocks in the immediate roof (shale and mudstone), forms a cave-in. Second layer of sandstone (II) experiences fracturing and displacement mostly in the vertical direction (but without the rotation of the fractured sandstone blocks). The breaking of the first layer of sandstone and the fracture of the second layer of sandstone is certainly the source of the low and medium-energy events. Table 5 lists all seismic activity which had occurred during the excavation of the longwall 729, grouped by the three segments of the longwall panel run: (1) from 0 m to 240 m; (2) 240 m-429 m and (3) 429 m-630 m. Most of events only had low and medium seismic energy present, whereas periodically, events with extremely large seismic energy appeared. After these events, a decision was made to reduce the speed of the exploitation from 5.2 m/day to 4.0 m/day and when the event with the seismic energy of $1.0 \cdot 10^9$ J had occurred at the 429 m advance, the speed was further reduced to 2 m/day in order not to squeeze the longwall. Simultaneously, torpedo blasting was performed from the longwall face at every 30 m of the advance and the amount of torpedo blasting drilled from the galleries was increased. Up to the 429 m longwall panel advance, the torpedo blasting was carried out only from the headgate

S-763 and tailgate S-712 in every 50m with the angle of 60°. They were drilled alternatively, one above the longwall panel and the other towards the fault or neighbouring longwall 728. Additional torpedo blasting was performed along the gallery S-770, corresponding to the already excavated panel 703, which is located in part S3, 60 m above. The length of each torpedo boreholes was 60 m and from 45 kg to 60 kg of explosive materials was used in each blast. In total, there were 109 torpedo blasts. The reduction of the longwall panel advance, together with the large number of the torpedo blasts, had resulted in a 130-fold decrease in the energy of seismic events and a significant rise in the number of low-energy events. The number of medium and large energy events diminished and extremely large energy events ceased. With an average excavation rate of 4.2 m/day, the average number of seismic events with low-energy (10^3 J, and 10^4 J) was 0.9 per meter of the longwall panel and at an excavation rate of 2 m/day this number increased to 2.1 per meter of the longwall. At the same time, the number of medium (10^5 J) and high (10^6 J) energy events had diminished as well. At an average excavation rate of 4.2 m/day, this value was 0.19 per meter of the longwall and at the speed of 2 m/day it was 0.13 per meter of the longwall.

TABLE 5

List of all seismic activity which had occurred during the longwall panel no. 729 excavation

Longwall panel advance no. 729	**Number of events and seismic energy released [J]**							**Total number of events**	**Sum of seismic energy**
	10^3	**10^4**	**10^5**	**10^6**	**10^7**	**10^8**	**10^9**	**[-]**	**[J]**
Up to 260 m	180	97	15	0	0	0	0	292	$3.9 \cdot 10^6$
From 260 m to 429 m	50	44	63	5	2	2	1	167	$2.6 \cdot 10^9$
From 429 m to 630 m	268	158	27	1	0	0	0	454	$2.0 \cdot 10^9$
Sum	498	299	105	6	2	2	1	913	$4{,}6 \cdot 10^9$

* At an advance of 260 m, the first event of a large magnitude had occurred with the energy of $2 \cdot 10^7$ J and at the 429 m advance, the strongest event had the energy of $1 \cdot 10^9$ J. Until this event, the longwall was excavated at an average rate of 4.2 m/day and the maximal progression per day was 6.75 m. Since then, the speed was reduced to 2 m/day.

Table 6 contains data related to the torpedo blasting, performed in order to reduce the risk of rock bursts in the vicinity of the longwall 729.

An analysis of Table 6 shows that:

a) Torpedo blasts performed in and around longwall panel 729 were very effective. After the detonation of 109 boreholes, the rock mass released a total seismic energy of $1.85 \cdot 10^6$J. This facts attests to the large stresses occurring in the longwall along the fault.

b) The face longwall blastings performed every 30 m were twice as effective as the blasts performed from the galleries adjoining the longwall. It is likely that this is because the area near the longwall face was under secondary stress influence as well, not only the initial stress.

c) The energy released after the torpedo blasts executed along the ramp S-770 of the longwall 703 (reaching over 100 m over longwall 729) was $2.1 \cdot 10^4$J per a borehole, which is similar to what was obtained during the blasts along the longwall 729 and the adjacent galleries. Notwithstanding the fact that the blasts were made in the 3rd sandstone layer (laying 85 m above the longwall 729), the results were similar to the blasts carried out in the roof 50 m above the longwall 729. Therefore, the torpedo blasts did not affect the 3rd layer of the sandstone (Fig. 4).

TABLE 6

Information on torpedo blasting carried out in the region

Longwall panel advance		Number of boreholes	Amount of explosives [kg]	Borehole length	Total seismic energy released* [J]	Total seismic energy released* per borehole [J]
From the start to 430 m		51	2787.0	2927.5	$4.6 \cdot 10^5$	$9.0 \cdot 10^3$
430 m	Gallery	9	538.5	1140	$1.3 \cdot 10^5$	$1.4 \cdot 10^4$
	Panel	7	373.5	420	$1.9 \cdot 10^5$	$2.7 \cdot 10^4$
460 m	Gallery	7	366.0	360	$1.3 \cdot 10^5$	$1.9 \cdot 10^4$
	Panel	7	411.0	429	$3.2 \cdot 10^5$	$4.6 \cdot 10^4$
487 m	Gallery	3	180.0	180	$4.0 \cdot 10^4$	$1.3 \cdot 10^4$
	Panel	6	378.0	366	$2.2 \cdot 10^5$	$3.7 \cdot 10^4$
515 m	Gallery	4	240.0	240	$0.3 \cdot 10^5$	$8.0 \cdot 10^3$
	Panel	6	378.0	366	$1.6 \cdot 10^5$	$2.7 \cdot 10^3$
541 m	Gallery	3	150.0	121	$0.6 \cdot 10^5$	$2.0 \cdot 10^3$
	Panel	6	378.0	366	$1.1 \cdot 10^5$	$1.8 \cdot 10^4$
Sum		109	6180	6915.5	$18.5 \cdot 10^5$	average $2.2 \cdot 10^4$ ·

* Energy released as the result of torpedo blasting

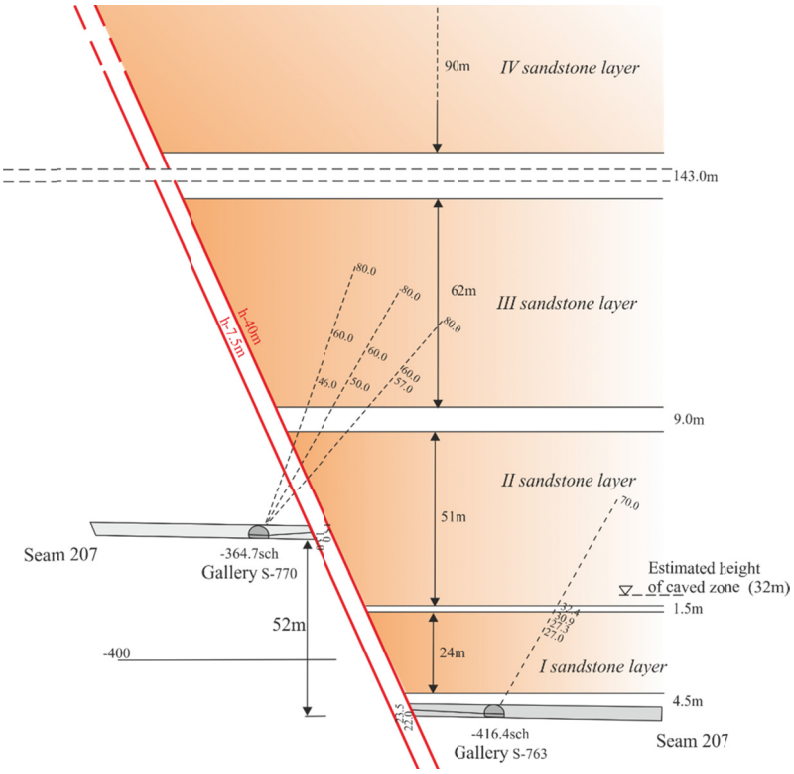

Fig. 4. Location of the thick layers of sandstones overburden the longwall panel 729 and the location of boreholes for torpedo blasts

The remaining question is that of the cause of the seismic events of the extremely large energy. Taking under consideration the seismic energy released in these events, which manifests itself on the ground surface but not in the area of the exploited seam, it appears that the causes can be found in layer III and layer IV of the sandstone in the vicinity of the fault. It can be said with a high degree of probability, that the extreme seismic energy events are a result of the fracturing of one of the two layers of the sandstone (mainly layer IV) in the vicinity of the "north" fault, as well as the sudden displacements at the fault. Table 7 presents information on the location of the longwall at the time the high energy events took place.

TABLE 7

Location of the longwall panel at the time the high energy events took place

Longwall panel no./ Part name	**Seismic energy of events, [J]**	**Date**	**Advance [m]**	**Distance from the previous event [m]**	**Distance from the gallery S-763 (Fig. 2), [m]**	**Distance from the longwall panel face, [m]**
Panel 700/ Part G	$3.0 \cdot 10^7$	21.03.2012	378 m	—		
Panel 729/ Part S_1	$2.0 \cdot 10^7$	18.09.2015	260 m	—	105 m	25 m from the longwall front, above the mining works
Panel 729/ Part S_1	$9.0 \cdot 10^8$	30.09.2015	300 m	40 m	105 m	20 m from the longwall front, above the mining works
Panel 729/ Part S_1	$5.0 \cdot 10^7$	10.10.2015	335 m	35 m	100 m	40 m from the longwall front, above the mining works
Panel 729/ Part S_1	$6.0 \cdot 10^8$	20.10.2015	378 m	43 m	–15 m	40 m from the longwall front (outside the wall)
Panel 729/ Part S_1	$1.0 \cdot 10^9$	18.11.2015	429 m	51 m	50 m	30 m from the long in the rock mass

The analysis of the results presented in Table 7 shows that the first event with the extremely large energy (with seismic energy $2 \cdot 10^7$ J) had occurred 260 m along the longwall, probably indicating the first fracture of the thick layer of the III and IV layer of the sandstone. Until then, only low and medium size events had taken place at this location of the longwall 729 (there were no events with seismic energy higher than 10^6 J) (Table 5): 180 events with the seismic energy of 10^3 J, 97 events with the seismic energy of 10^4 J, 15 events with the seismic energy of 10^5 J.

The cause of these events is probably due to the fracturing of layer I of the sandstone with the thickness of 24 m, laying 4.5 m above the seam 207, as well as the fracturing of layer II of the sandstone with the thickness of 51 m, lying 30 m above seam 207. These layers were fractured periodically, due to a network of small faults with small throws, not exceeding 2.2 m and occurring in the longwall panel.

After the first event of the extremely large seismic energy had occurred ($2 \cdot 10^7$ J), four such events with seismic energies: $9.0 \cdot 10^8$ J; $5.0 \cdot 10^7$ J; $6.0 \cdot 10^8$ J; $1.0 \cdot 10^9$ J, took place regularly,

every 45 m of the longwall length (the average distance between events was computed taking into account its energy – see Table 7). These events should be linked with the fracturing of layer III and IV of the sandstone, accompanied with the fault displacement. One can hypothesize that these high-seismic energy events are a result of the combination of the following four conditions:

1. The presence of the "north" normal fault with an inclination of about $\alpha = 68°$, an average throw of 52 m, and the associated high initial horizontal stress perpendicular to the "north" fault.
2. The negative impact of the longwall panel 703 in the sector S3, which lies parallel to the "north" fault at a distance from 15 m to 40 m. The first event of the extremely large magnitude ($2 \cdot 10^7$J) had occurred when the horizontal distance between the face of the longwall 729 and the closest corner of goaf (no. 703) was 110 m. Further events had occurred when this distance was 70 m – the event with seismic energy $9 \cdot 10^8$ J, 40 m – the event with the seismic energy of $5 \cdot 10^7$ J, 0 m – event with the seismic energy of $6 \cdot 10^8$ J and 30 meters behind the goaf corner: $1 \cdot 10^9$ J. Therefore, the greatest danger of the extreme seismic events had occurred between the 260 m and 429 m advance of the longwall panel.
3. The existence of four thick layers of porous sandstone with low strength parameters, similar to shale, which fractures easily, in the roof above.
4. The exploitation of the higher level seams: no. 116/2 in the years 1968-1992; no. 117 in the years 1968-1994; no. 118 in years 1970-1996 and no. 119/2 in the years 1976-1909. The exploitation of the seam 119/2 had a large impact on the sandstone layer IV because it is located directly above that layer. Its exploitation surely led to the fracturing of the upper part of the layer IV of the sandstone to a depth of 15-20 m, as well as a significant change in its state of stress at a depth of 50-60 m (Borisow, 1980).

This mechanism is also confirmed by the course of the displacements which had taken place at the surface (McGarr and Bicknell, 1990). After the exploitation in neighbouring mines, discontinuous deformations had formed on the surface in the vicinity of fault (unfortunately above longwall 729 no surface displacement measurements were performed). In Tajduś et al. (2016), a numerical simulation was used to compute the critical value of the friction coefficient above which the fault displacement does not take place for normal faults with different slopes. The critical value can be computed with:

$$\mu_{kr} = \frac{1}{\tan(\alpha)}\left[\frac{0.0128 \cdot E + 1.221}{\nu} - 1.935\right] \tag{2}$$

Substituting into formula 2 the estimated values $\alpha = 68°$, $E = 3$GPa, $\nu = 0.25$, one obtains $\mu_{kr} = 1.25$ for the rock mass in the fault region. Above this value, there is no displacement along the fault. From the literature (Byerlee, 1978), the friction coefficient along a fault can be estimated as $\mu = 0.85$, which means that it is lower than the coefficient value under which the displacement along the fault is possible. Therefore, propitious conditions had existed for a sudden displacement along the fault during the exploitation of the longwall panel 729 on the seam 207.

Figure 5 schematically shows the extent of the influence of the exploitation of the panel 729, together with the direction of the north fault. At a vertical distance H_1 from the longwall 729, the range of influence of the exploitation is cut off by the fault. The Budryk-Knothe theory (Knothe; 1953, 1984) was used to calculate the influence of the exploitation on the rock mass. Knowing

the angle of the main influence β and the fault inclination angle α, one can compute the vertical distance H_1 from the exploited longwall, above which the fracturing of the thick layer of sandstone most likely occurs. The formula is:

$$H_1 = s_i \frac{\tan(\alpha)\cdot\tan(\beta)}{\tan(\alpha)-\tan(\beta)} \tag{3}$$

where:

- β — angle of main influence, (for presented conditions $\beta = 62°$),
- α — average inclination of north fault ($\alpha = 68°$),
- s_i — width of the i-th pillar between the panel and the fault, (for panel no. 729, the average value is $s_1 = 30$ m).

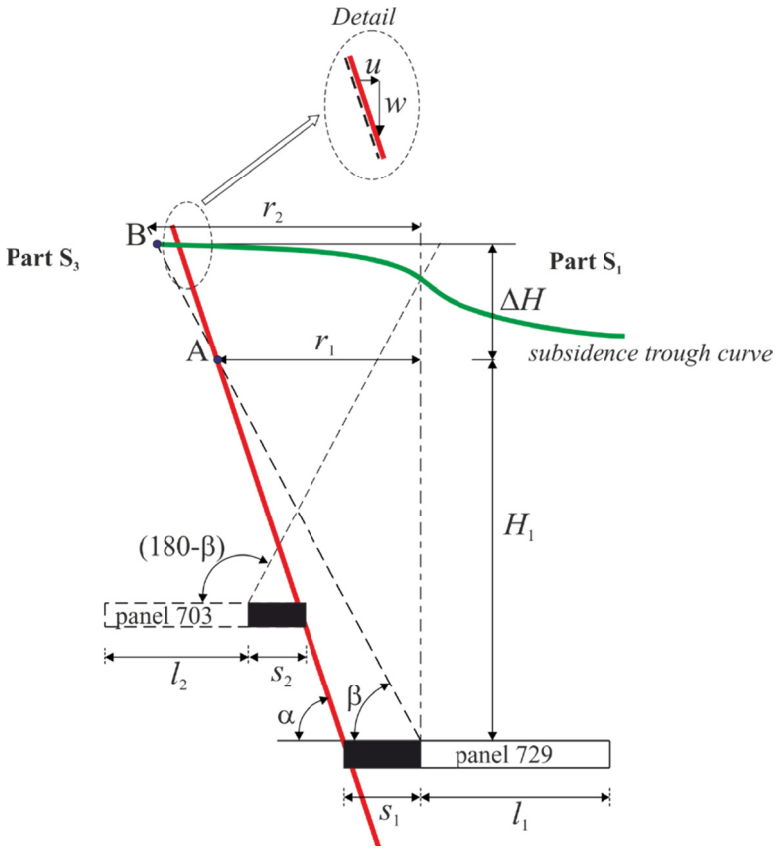

Fig. 5. Radius of the main influence range for the longwall panel 729 together with the direction of the north fault

Substituting the values into the equation (3), a height of $H_1 = 235$ m is obtained (425 m from the ground level). The fracture of sandstone occurs higher ($H_1 + \Delta H_1$), at a horizontal distance "x"

from the fault. As a result of the fracture, a sudden displacement on the fault occurs, as well as a substantial energy release. Previous experiences from other mines show that following a high-energy event at the fault outcrop, a discontinuous displacement may occur in the form of a fault with a small throw, eg. up to 0.6 m (Celmer et al., 2012), indicating displacement within the fault.

5.4. Numerical calculations of the surroundings of the fault

In order to determine the state of stress and strain in the vicinity of the fault during the excavation of the longwall panels 703 and 729, numerical calculations were made for a flat cross-section perpendicular to the fault (at a length of 429 m for longwall 729) as shown in Fig. 6.

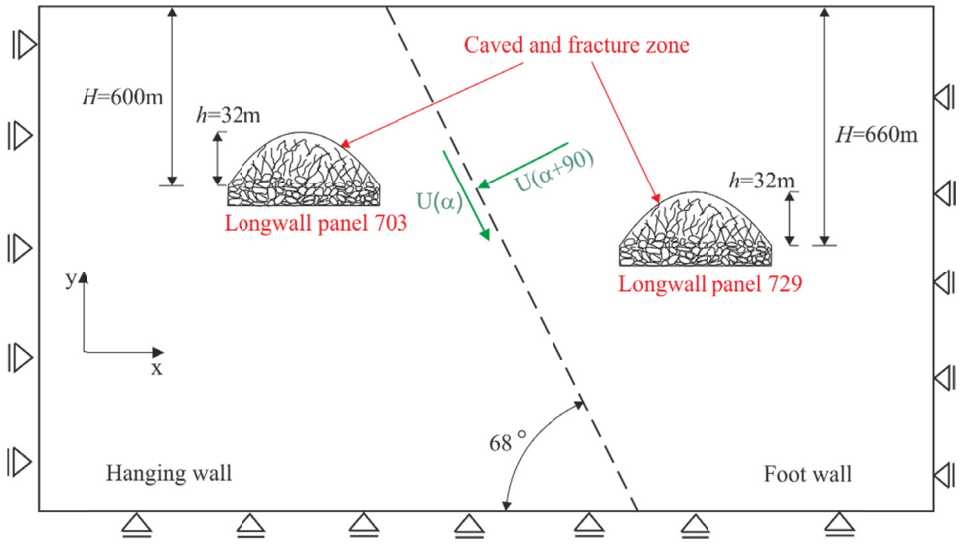

Fig. 6. The geomechanical model used in the calculations

In the model, the average values of the deformation parameters for the overburden were: $E = 3.0$ GPa, $\nu = 0.25$, $\gamma_{vol} = 0.025$ MPa/m. It was assumed that above the excavated panels, the caved and fracture zones are formed and reach 32 m. Two numerical calculations were performed. In the first, it was assumed that only one panel 703 was excavated, while in the second, both longwalls 703 and 729 were excavated. Shown in Fig. 7 is the variation of the displacement occurring at the "north" fault at the footwall and the hanging wall blocks, following the excavation of the longwall 703. Figure 8 shows the displacements which had occurred on both sides of the "north" fault, following the excavation of longwalls 703 and 729. Table 6 contains the values of displacement at the "north" fault at selected depths.

The results show a difference in displacement between the footwall and the hanging wall blocks of about -0.05m (discontinuous displacements), following the excavation of the longwall 703, as well as the excavation of longwalls 703 and 729. As the depth increases, the difference in the displacement between the hanging wall block and the footwall block decreases following for the first step. At a depth of about 460 m (140 m above seam 703), this difference

reduces to zero and the displacements at the fault (shown in Table 8) become larger for the footwall block. A similar behaviour is observed at the fault following the excavation of both longwalls 703 and 729. For this case, however, the difference in displacement along the fault between the hanging and footwall blocks occur much more rapidly. As the depth increases, the difference diminishes rapidly and at a depth 350 m (300 m above seam 729) it reduces to zero. An increase in displacement can be seen from the footwall with respect to the displacements at the hanging wall block.

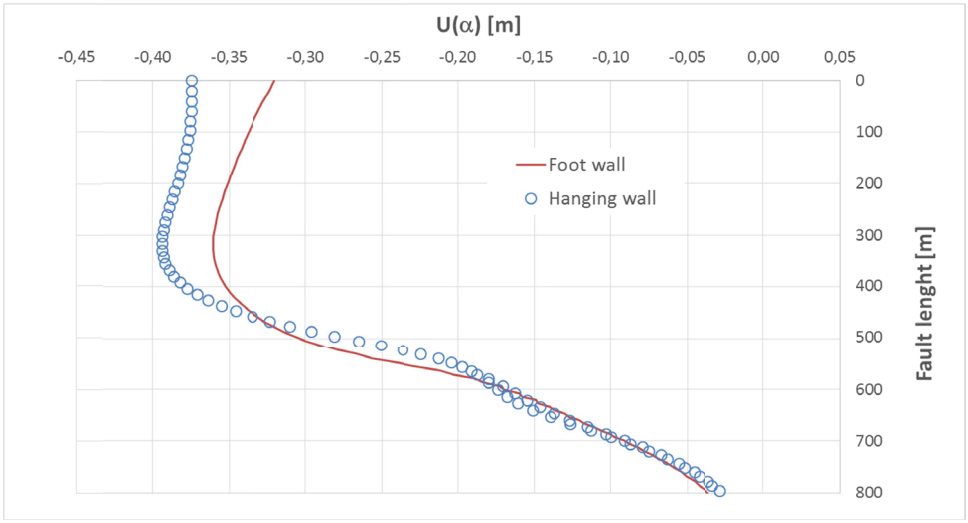

Fig. 7. Displacements at the "north" fault $U(\alpha)$ following the excavation of longwall 703

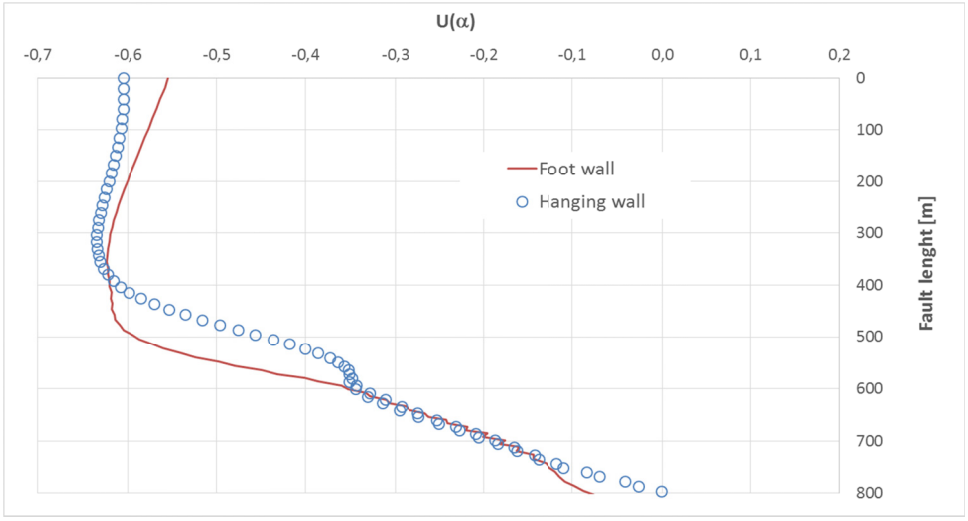

Fig. 8. Displacements at the "north" fault $U(\alpha)$ following the excavation of longwalls 703 and 729

TABLE 8

Displacements occurring at the "north" fault at selected depths

H [m]	Mining activity at the longwall panel 703			Mining activity at longwalls 703 and 729		
	Hanging wall $U(\alpha)_H$ [m]	Foot wall $U(\alpha)_F$ [m]	Difference in displacement [m]	Hanging wall $U(\alpha)_H$ [m]	Foot wall $U(\alpha)_F$ [m]	Difference in displacement [m]
0	–0.375	–0.321	–0.054	–0.605	–0.555	–0.050
200	–0.386	–0.353	–0.033	–0.624	–0.604	–0.020
250	–0.392	–0.359	–0.033	–0.633	–0.616	–0.017
300	–0.394	–0.361	–0.033	–0.635	–0.622	–0.013
350	–0.387	–0.356	–0.031	–0.623	–0.622	–0.001
400	–0.378	–0.341	–0.037	–0.570	–0.618	+0.048
450	–0.296	–0.314	–0.018	–0.476	–0.604	+0.128
500	–0.213	–0.257	0.044	–0.373	–0.524	+0.151

Shown in Fig. 9 is the variation of the strain along the fault between the hanging wall and the footwall blocks, following the excavation of the longwall 703 and the excavation of both longwalls 703 and 729. Figure 10, on the other hand, depicts the variation of the strain acting perpendicular to the fault, between the hanging wall and the footwall blocks for both of the analysed cases. The strain difference changes significantly with depth, and reaches maximal values at two locations. Table 7 shows the maximal values for the strain difference and the depths at which they occur.

TABLE 9

The maximal values for the strain difference

Mining activity at the longwall panel 703			Mining activity at longwall panels 703 and 729		
H [m]	$\Delta\varepsilon(\alpha)_{max}$	$\Delta\varepsilon(\alpha+90)_{max}$	H	$\Delta\varepsilon(\alpha)_{max}$	$\Delta\varepsilon(\alpha+90)_{max}$
470 m	$4.6\times10^{-0.4}$	$1.4\times10^{-0.4}$	420 m	$1.0\times10^{-0.3}$	$3.1\times10^{-0.4}$
510 m	$-4.9\times10^{-0.4}$	$-2.5\times10^{-0.4}$	520 m	$-1.8\times10^{-0.3}$	$-5.3\times10^{-0.4}$

From the analysis of the strain variation at the fault between the foot wall and the hanging wall, the following conclusions can be drawn:

- The maximal strain difference values from Table 9 correspond to either tension or compression, depending on the depth.
- The tensile strains at the fault represent a particular rock burst hazard. Such conditions can result in the release of a substantial amount of energy and in a sudden displacement at the fault. During the excavation of the longwall 729, the maximal difference in the tensile strains occurs along the fault ($1.0\times10^{-0.3}$) and in the perpendicular direction to it ($3.1\times10^{-0.3}$) at a depth of about 420 m (i.e. 240 m above the longwall 729). This difference is twice as large as the one encountered during the excavation of longwall 703, where no events of an extremely large magnitude had occurred.

The maximal difference in the compressive strains occurs at a depth of about 520 m. Its absolute value is larger than the maximal tensile strain difference. The compressive strains occur along the length fault, and also in the direction perpendicular to it. Such conditions do not lead to sudden displacements at the fault nor to the creation of a high-energy seismic event at this location.

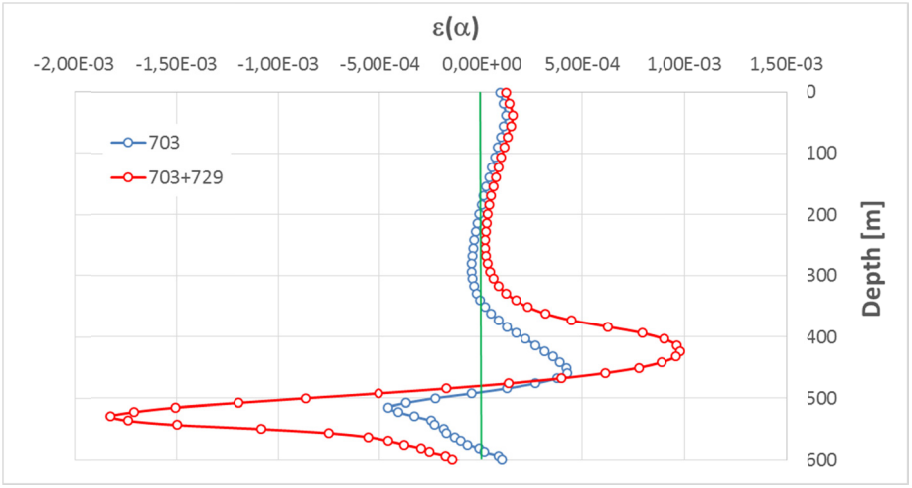

Fig. 9. Strain difference $\Delta\varepsilon(\alpha)_{max}$ between the foot wall and the hanging wall, following the exploitation of the longwall 703 (in blue) and longwalls 703 and 729 (in red)

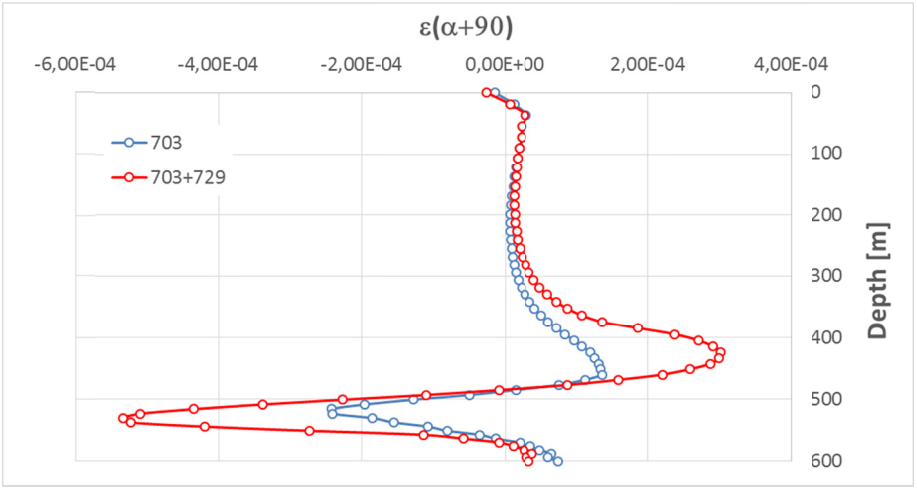

Fig. 10. Strain difference $\Delta\varepsilon(\alpha + 90)_{max}$ between the foot wall and the hanging wall, following the exploitation of the longwall 703 (in blue) and longwalls 703 and 729 (in red)

6. Conclusions

The causes of the seismic events of an extremely large energy, which had occurred during the excavation of the longwall 729 at the "north" fault, were examined. Furthermore, methods were presented in order to avoid rock bursts in the vicinity of the fault zone. The results of the analysis indicate that the cause for the seismic events during the excavation of the longwall panel 729 is the sudden displacements at the "north" fault at a depth of about 400 m and the fracture

at the IV layer of sandstone. Similar situations occur during the exploitation of other coal mines along the Vistula River in the Upper Silesia region in Poland. Although the seismic events do not cause damage to the mines themselves, they are, however, strongly felt at the surface. From the analysis conducted hereby, it is possible to identify one of the principal factors of the occurrence of such events, namely, the activation of the faults due to the mining activity in the close proximity. During the design of the mining activity in a fault zone, it is assumed that the distance from the fault should not be smaller than 30 m. In order to reduce the seismicity hazard, this distance should be increased and should not be smaller than 45 m, which is due to both the location of the events and the energy released.

References

Borisow A.A., 1980. *Mechanika gornych porod i massiwow*. Izdatelstwo Niedra, Moskwa (in Russian).

Byerlee J., 1978. *Friction of Rocks*. Birkhauser Verlag, Pageoph. **116**, 615-626.

Celmer M., Lubryka M., Kutkowski J., 2012. *Problemy z praktyki kopalnianej w zakresie określania wpływu uskoków na budynki znajdujące się na powierzchni terenu*. Górnictwo i Geologia **7**, 1 (in Polish).

Coughlin J., Kranz R., 1991. *New Approaches to Studying Rock Burst-Associated Seismicity in Mines*. The 32nd U.S. Symposium on Rock Mechanics (USRMS), 10-12 July, Norman, Oklahoma.

Guoa W.-Y., Zhaoa .T-B., Tan Y.-L., Yua F.-H., Hua S.-C., Yangc F.-Q., 2017. *Progressive mitigation method of rock bursts under complicated geological conditions*. International Journal of Rock Mechanics & Mining Sciences **96**, 11-22.

Kidybiński A., 1981. *Bursting liability indices of coal*. Int. J. Rock Mech. Min. Sci. Geomech. Abs. **18** (4), 295-304

Knoll P., Kuhnt W., 1990. *Seismological and technical investigations of the mechanics of rock burst*. Rockbursts and Seismicity in Mines, 129-138.

Knothe S., 1953. *Równanie profilu ostatecznie wykształconej niecki osiadania*. Archiwum Górnictwa i Hutnictwa (Archives of Mining Sciences) **1**, 1 (in Polish).

Knothe S., 1984. *Prognozowanie wpływów eksploatacji górniczej*. Wyd. Śląsk. Katowice (in Polish).

Mutke G., Dubiński J., Lurka A., 2015. *New criteria to assess seismic and rock burst hazard in coal mines*. Archive of Mining Sciences **60**, 3, 743-760. DOI: 10.1515/amsc-2015-0049

McGarr A., Bicknell J., 1990. *Estimation of the near – fault ground motion of mining – induced tremors from locally recorded seismograms in South Africa*. Rockbursts and seismicity in mines, 245-248.

Peng S., 2006. *Longwall Mining*. Second Edition, Morgantown, University Press.

Staroń T., 1979. *Eksploatacja pokładów węgla z zawałem stropu w sąsiedztwie pól pożarowych*. Katowice, Wyd. Śląsk (in Polish).

Tajduś A., Cała M., Tajduś K., 2016. *The influence of normal fault on initial state of stress in rock mass*. Studia Geotechnica et Mechanica **38**, 1, 109-121.